Multilayered Beam, Plate and Shell Theories with Interlaminar Variables and Lagrange Polynomials

MEMORIE

DELL'ACCADEMIA DELLE SCIENZE DI TORINO

1

SERIE VI

2022

Estratto

ACCADEMIA·DELLE·SCIENZE·DI·TORINO
VERITAS·ET·VTILITAS
R·SCIENT·TAVRIN·ACADEMIA
INSTAVRATA
MDCCLXXXIII

Acc. Sc. Torino
Memorie 1 (2022), 99-134, 23 figg., 11 tabb. SCIENZA DELL'INGEGNERIA

Multilayered Beam, Plate and Shell Theories with Interlaminar Variables and Lagrange Polynomials

Erasmo Carrera[*], Riccardo Augello[**]
e Daniele Scano[***]

Memoria presentata dal Socio corrispondente Erasmo Carrera
nell'adunanza del 9 febbraio 2022, ricevuta il 4 marzo 2022
e approvata nell'adunanza del 18 maggio 2022

Abstract. *This paper proposes Finite Elements (FEs) based on Lagrange polynomials for the static analysis of multilayered one-dimensional beams and two-dimensional plates and shells. Lagrangian Mechanics (LM) is recalled as the starting point for the development of the Carrera Unified Formulation (CUF), which is adopted to derive FE matrices. In addition, CUF allows accounting for the assumption of any theory order, e.g., any choice of Lagrange Points (LPs) through the layers, mainly values at the interfaces. FEs are developed in the framework of the so-called Equivalent Single Layer (ESL) modellings, and the results are compared to the more traditional and more computationally expensive Layer-Wise (LW) approaches. Four well-known benchmarks are considered to assess the capability and effectiveness of the proposed ESL beam, plate and shell FEs. Results clearly demonstrate the reliability of the models for the evaluation of displacements and both in-plane and shear stresses. Finally, the advantages of theories based on Lagrange polynomials formulations to deal with non-classical geometrical boundary conditions and global-local approaches are discussed.*

Keywords: Lagrange Polynomials, Unified Models, Multilayered Beams, Plates and Shells, Finite Element Method, Carrera Unified Formulation.

[*] Politecnico di Torino; erasmo.carrera@polito.it

[**] Politecnico di Torino; riccardo.augello@polito.it

[***] Politecnico di Torino; daniele.scano@studenti.polito.it

Riassunto. *Questo articolo propone alcuni Elementi Finiti (FEs) basati sui polinomi di Lagrange per l'analisi statica di travi, piastre e gusci multistrato. La meccanica Lagrangiana (LM) è richiamata come il punto iniziale per lo sviluppo della* Carrera Unified Formulation *(CUF), la quale è adottata per derivare le matrici degli Elementi Finiti. Inoltre, la CUF permette di considerare assunzioni per teorie di ogni ordine; ad esempio, qualsiasi scelta dei punti di Lagrange (LPs) attraverso gli strati. Gli elementi finiti sono sviluppati nel contesto del cosiddetto approccio* Equivalent Single Layer *(ESL), e i risultati sono confrontati con quelli più onerosi noti come approcci* Layer-Wise *(LW). Quattro problemi campione sono considerati per valutare la capacità ed efficacia degli elementi finiti ESL travi, piastre e gusci. I risultati dimostrano la robustezza dei modelli per il calcolo degli spostamenti e delle tensioni nel piano e trasverse. Infine, sono discussi i vantaggi delle teorie basate sulle formulazioni con i polinomi di Lagrange per trattare condizioni al contorno geometriche non classiche, dimostrandone il vantaggio in analisi* global-local.

Parole chiave: metodo degli elementi finiti, modelli unificati, piastre e gusci, polinomi di Lagrange, travi multistrato.

1. Introduction

In the last decades, multilayered structures have been used in many applications, e.g., in aerospace, naval and automotive fields. The continuous development of sophisticated components led to increasingly complex designs that require reliable analyses, which main issue is represented by the anisotropy of such structures, causing complex mechanical phenomena. For instance, the shear stresses must fulfil interlaminar continuity and transversely discontinuous mechanical properties cause the zig-zag distribution of displacement fields.

In [1], these effects were referred to as C^0_z-requirements. The coupling between the in-plane and out-of-plane strains also represents a challenging topic. An overview of several computational techniques for the analysis of one-dimensional (1D) and two-dimensional (2D) structures can be found in major review articles, see [2, 3] and [4, 5], respectively. However, a brief discussion about some noteworthy contributions in the field is given hereafter for the sake of completeness. Classical theories such as the Euler-Bernoulli Beam Model (EBBM) [6], and Timoshenko Beam Model (TBM) [7] are still widely applied in numerical simulations, although they

lack the ability to accurately evaluate the shear strain components, which are considered null by EBBM and constant by TBM. When dealing with thin-walled structures, whose cross-sectional deformation is relevant, an accurate evaluation of the stress distribution is necessary to describe the higher-order phenomena. For this reason, classical approaches may be inappropriate and lead to wrong conclusions, and advanced structural theories must be considered, see the classical book by Novozhilov [8]. Vlasov [9] introduced warping functions to capture the deformations of beam cross-sections. This approach found great success among scientists, see the works by Ambrosini *et al.* [10], Mechab *et al.* [11] and Friberg [12], who made use of warping functions for thin-walled structures. The so-called Generalized Beam Theory (GBT) was suggested by Schardt [13]. GBT allows the displacement field to be expressed as a linear combination of cross-sectional deformation modes. This theory was adopted by Peres *et al.* [14] for the analysis of curved thin-walled beams, and by Silvestre [15] for buckling problems.

As far as the 2D plate and shell problems are concerned, the classical 2D model is represented by Kirchhoff-Love theory [16, 17], whose extension to laminates is known as the Classical Lamination Theory (CLT) [18]. CLT neglects the effect of out-of-plane strains and some drawbacks can surge for practical studies. On the other hand, First Shear Deformation Theory (FSDT), which is based on the works by Reissner [19] and Mindlin [20], accounts for the shear deformation effects by linear variation of in-plane displacements and it still plays a key role in commercial codes. In order to overcome the limitations of classical theories, several refined plate Finite Elements (FEs) were developed over the last years. For instance, see the one developed by Reddy [21], the so-called zig-zag theories [1], the theories based on the Reissner's Mixed Variational Theorem (RMVT) [5]. Most of the works discussed so far are based on an Equivalent Single Layer (ESL) approximation of the laminate. In ESL models, the variables are independent of the number of layers. On the other hand, a detailed analysis may require the adoption of Layer-Wise (LW) models, where the number of unknowns depends on the number of layers (see Carrera [22]). FE implementations of LW theories were proposed by many authors, such as for example Rammerstorfer *et al.* [23], Reddy [24], Mawenya and Davies [25], and Noor and Burton [26]. However, the enhanced accuracy of LW models demands high computational costs. A review of the theories for the analysis of anisotropic multilayered plates was proposed by Carrera [27] and by Carrera and Robaldo [28] for thermo-piezoelasticity.

Several efforts were addressed by researchers to make the composite beam, plate and shells models as accurate as efficient. An example is the concept of selective ply grouping or sublaminates [29, 30, 31], in which some local regions are created over the plate and shell thickness, identified by specific ply or plies, where LW theories are applied. On the other hand, in the global region, which is the portion of the domain where accurate analysis is not needed, lower-order and eventually ESL models can be adopted. Both ESL and LW models may eventually be implemented by using a combination of Lagrange and Legendre polynomials for formulate the kinematics theory over the thickness.

In this manner, the continuity of the variables between local and global regions can be immediately satisfied. In the work by Botshekanan Dehkordi *et al.* [32], a variable kinematics description in the thickness direction for the static analysis of sandwich plates was performed. That model was derived in the framework of the Carrera Unified Formulation (CUF) and Reissner-Mixed-Variational-Theorem (RMVT) was adopted for an *a-priori* evaluation of the transverse shear and normal stresses. Thus, the transverse stresses were approximated using a mixed LW/ESL approach. Adopting the principle of virtual displacements, Carrera and Valvano [33] implemented variable kinematics shell models for laminated structures with embedded piezoelectric components using Legendre polynomials. Instead, Lagrange polynomials are used for beam and plate and shell formulations in Pagani *et al.* [34].

A method to further reduce the computational costs, while keeping a high level of accuracy, is the adoption of global/local techniques. They were developed especially for composite materials, see [35]. Among these methods, particular attention is dedicated to the so-called «multi-steps methods», in which the local analysis of the zone of interest requires the boundary conditions at the interface level that are obtained by the analysis of the global structure. For instance, the global/local methodology proposed by Mao *et al.* [36] makes use of a coarse mesh to analyse the entire structure and to obtain the nodal displacements, which were subsequently applied as boundaries to the refined local model. According to [36], the application of the boundary conditions in the local region inevitably introduces errors. To minimize the effect of such errors, the local analysis generally requires a larger region than the critical one, where accurate stress fields need to be evaluated. In the framework of CUF, a two-step global/local methodology can be built (see [37, 35, 38]). The first step is devoted to the static analysis of a global model of the structure and it could

be done by commercial software using 1D or 2D elements. A criterion is established to identify the most critical region, which is subsequently analyzed in the second step by using high-order models, to obtain accurate stress fields. The refined theories used in the detailed analysis are implemented in the framework of CUF. Another class of methods concerns the coupling of "refined" and "coarse" subdomains. Dhia [39] and Dhia and Rateau [40] suggested the Arlequin method to enforce compatibility within the overlapping domain with Lagrange multipliers. The Arlequin method was implemented in the framework of CUF by Biscani *et al.* [41] for 1D and 2D models [42]. He *et al.* [43] adopted the Arlequin method to bridge low- and high-order models constructed with CUF, and the Constrained Variational Principle (CVP) was used to derive beam elements for multi-layered structures with individual kinematics in each layer. Similar results were reproduced by Carrera *et al.* [44, 45] by coupling models with different kinematics by using point-wise Lagrange multipliers. The two methods differ since the first one needs an overlapping region between the sub-domains.

This paper wants to establish and detail the advantage of adopting the Lagrange polynomial for the construction of finite elements of beams, plates and shells.

The main advantages of Lagrangian approach are the following:

– The user can choose the number of Lagrange Points (LPs) and their position, within the domain of the thickness in the case of plates and shells and the cross-section in the case of beams, without altering the results;
– The unknowns at every LP are pure displacements, and it is possible to use different boundary and congruence conditions.

This paper is structured as follows: Section 2 gives a brief introduction about the Lagrangian Mechanics (LM) as a starting point for CUF formalism, followed by a description of the proposed approach for the modelling of multilayered beams, plates and shells in Section 3. Section 4 describes the CUF form of the beam, plate, shell assumptions while Section 5 introduces the related FEs description. Section 6 describes the four case studies analyzed in this work, whereas the ESL numerical results, in terms of displacements and axial and shear stresses, are given in Section 7. In Section 8, meaningful examples are presented to assess the validity of the proposed ESL Lagrange

approach for changing boundary conditions and global/local methodology. Finally, the conclusions of this work are drawn.

2. Lagrangian mechanics and CUF

Two popular approaches for the analysis of structures are represented by the Newtonian and Lagrangian Mechanics (LM). The former considers the "equilibrium" of the forces, internal and external, acting on the body. For instance, let us consider a generic bar structure with constant cross-section and isotropic and homogeneous material subjected to an external traction force and a distributed axial force, as depicted in Fig. 1.

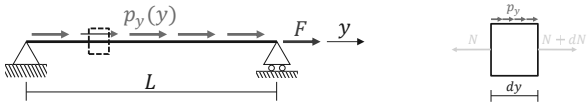

FIGURE 1 – *Generic bar with constant cross-section and isotropic and homogeneous material subjected to an external traction force and a distributed axial force.*

The equilibrium along the y direction can be written as

$$N_{,y} = -p_y \tag{1}$$

where $N = \int \sigma_{yy}\, dA$ is the internal axial force, with A being the area of the cross-section, σ_{yy} the axial stress coming from the Hooke's law $\sigma_{yy} = E\, \varepsilon_{yy}$, E the Young modulus and $\varepsilon_{yy} = v_{,y}$. Finally, p_y is the applied distributed loading. In the case of LM, the principle of virtual work is introduced and applied to the proposed problem:

$$\delta L_{int} = \delta L_{ext} \tag{2}$$

The choice of the Degree Of Freedom (DOF), to be used in Eq. (2), needs to be taken. In this application, the displacement along the axial direction is selected, and it is considered constant over the cross-section (x, z) of the bar in Fig. 1. As a consequence, the unknown displacement and its variation are

$$\begin{aligned} v(x,y,z) &= v^0(y), \\ \delta v(x,y,z) &= \delta v^0(y) \end{aligned} \tag{3}$$

The two terms of Eq. (2) can be written as follows :

$$\begin{aligned}\delta L_{int} &= \int_{\mathrm{V}} \sigma_{yy}\delta\varepsilon_{yy}\mathrm{dV} = \int_0^{\mathrm{L}} \mathrm{A}\sigma_{yy}\delta\varepsilon_{yy}\mathrm{d}y = \int_0^{\mathrm{L}} N\delta\varepsilon_{yy}\mathrm{d}y = \int_0^{\mathrm{L}} N\delta v^0_{,y}\mathrm{d}y \\ \delta L_{ext} &= \int_0^{\mathrm{L}} p_y\delta v^0(y)\mathrm{d}y\end{aligned} \tag{4}$$

where V is the volume of the structure. Introducing Eq. (4) into Eq. (2), upon integration by parts (see [46] for details), the following relation is obtained (boundary condition terms are omitted for the sake of brevity) :

$$\delta v^0 : N_{,y} = -p_y \tag{5}$$

which clearly states that the LM leads to the governing equations consistent to the choice made at Eq. (3).
The process of making assumptions can be generalized and written in a unified manner, including the DOFs related to the cross-sectional displacement, as follows (this would consist in a beam case) :

$$\begin{array}{lcll}\mathbf{u}(x,y,z) & = & F_\tau(x,z)\mathbf{u}_\tau(y), & \tau = 1,...,M \\ \delta\mathbf{u}(x,y,z) & = & F_s(x,z)\delta\mathbf{u}_s(y), & s = 1,...,M\end{array} \tag{6}$$

where $\mathbf{u}(x,y,z) = \{u,v,w\}^{\mathrm{T}}$, M is the number of terms of the expansion function $F_\tau(x,z)$ and $F_s(x,z)$ and the summing convention with the repeated indexes τ and s is assumed. [1]
Equation (6) represents the starting point for the Carrera Unified Formulation (CUF). Using Eq. (2), the description of the static problem results in the resolution of the following relation written in the strong form:

$$\delta\mathbf{u}_s : \ \mathbf{K}^{\tau s}\,\mathbf{u}_\tau = \mathbf{P}_s \tag{7}$$

The boundary conditions equations have to be added to Eq. (7), as detailed, for instance, in [47]. The unified formulation is described and adopted in this work to build beam, plate and shells models.

[1] Considering the v displacement only and $N = 1$, $N = F_\tau(x, z) = F_s(x, z) = 1$, $v_\tau(y) = \mathrm{v}^0(y)$ and $\delta v_s = \delta v^0$, Eq. (6) is reduced to Eq. (3).

3. Use of Lagrange Polynomials in theory of structures.

The advantages of adopting Lagrange polynomials for the structural analysis are discussed in this section. We start with one-dimensional beam structures.

3.1. The case of homogeneous beams

The properties and possibility of Lagrange polynomials are considered in the following bullets.

— Placement of unknown variables. Considering a generic beam structure as depicted in Fig. 2(a) and applying TBM in Fig. 2(b), the three-dimensional displacement field is evaluated as follows

$$\begin{array}{lcl} u(x,y,z) & = & u_1^0(y) \\ v(x,y,z) & = & v_1^0(y) + z\phi_{x1} - x\phi_{z1} \\ w(x,y,z) & = & w_1^0(y) \end{array} \tag{8}$$

The system of equations described in Eq. (2) has five unknowns. The

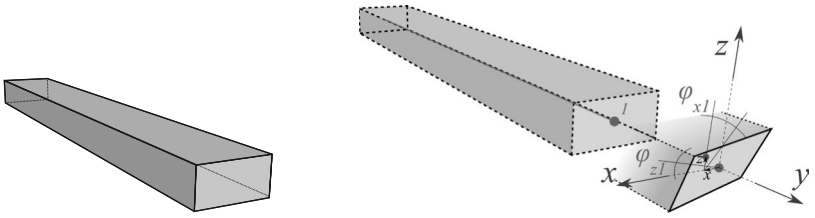

FIGURE 2 – *Generic beam structure (a) and Timoshenko Beam Theory (b).*

structure depicted in Fig. 2(a) can be described using Lagrange polynomials, and the corresponding LPs can be put as described in Fig. 3 in order to replicate the situation described by the classical approach (Fig. 2(b)). The resulting system of equations is then

$$\begin{array}{lcl} u(x,y,z) & = & u(y) \\ v(x,y,z) & = & L_1 v_1(y) + L_2 v_2(y) + L_3 v_3(y) + L_4 v_4(y) \\ w(x,y,z) & = & w(y) \end{array} \tag{9}$$

where L_1, L_2, L_3 and L_4 are the Lagrange polynomials evaluated at the

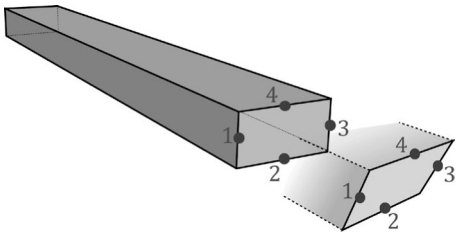

FIGURE 3 – *Generic beam structure with the Lagrangian approach.*

corresponding LPs. Then, the capability of LM to be valid for every point can be exploited, and the position of them can be changed to describe the geometry of the cross-section, as described in Fig. 4.

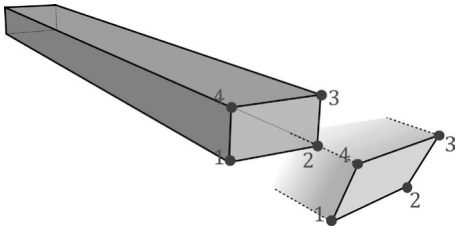

FIGURE 4 – *Generic beam structure with Lagrangian approach exploiting the capability of localization of LPs.*

— **The problem variables are pure displacements.** Referring to Fig. 4, the kinematic of the cross-section can be enriched as described in the following relations:

$$\begin{array}{lcl} u(x,y,z) & = & L_1u_1(y)+L_2u_2(y)+L_3u_3(y)+L_4u_4(y) \\ v(x,y,z) & = & L_1v_1(y)+L_2v_2(y)+L_3v_3(y)+L_4v_4(y) \\ w(x,y,z) & = & L_1w_1(y)+L_2w_2(y)+L_3w_3(y)+L_4w_4(y) \end{array} \tag{10}$$

The resulting system of equations has 12 unknowns, which are the displacements on the three directions of the four LPs laying on the cross-section. This leads to a heavier model (more DOFs), but allows for the description of the cross-section in-plane deformation.

— **Application of boundary conditions.** Boundary conditions can be used as kinematic constraints in correspondence of each LP. As a consequence, it is possible to use boundary conditions also in the longitudinal

edges (see [48]). An example is given in Fig. 5.

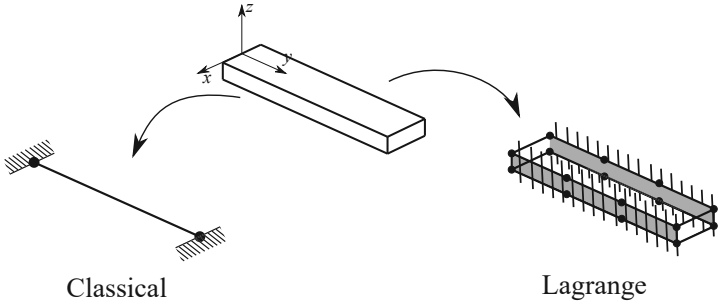

FIGURE 5 – *Boundary condition application with classical approach and Lagrange polynomial.*

3.2. The case of multilayered structures

Multilayered structures are characterized by the so-called C_z^0 requirements [1], that is the displacements and shear stresses are step-wise continuous in the thickness direction of the laminate. As depicted in Fig. 6, LPs can be used at the interface between two layers, and since the unknowns are pure displacements, the C_z^0 requirements are satisfied. If a given Lagrange polynomial is used in

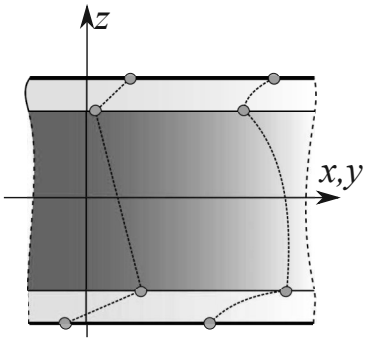

FIGURE 6 – *Application of LPs at the interlaminar level of a composite structure.*

each layer, the so-called Layer-Wise (LW) approach is obtained, where every

layer has its kinematics independently described. This approach leads to accurate results, but it could result more computationally expensive. An alternative technique is that known as the Equivalent Single Layer (ESL). Basically, it homogenizes every layer into an equivalent one, which properties are obtained as a combination on those of the layers. In the present work the efficiency of ESL models based of Lagrange polynomials is proposed.
The capability of the placement of unknown variables allows for the adoption of the points in any position of the structure. Figure 7 reports a domain of a four-layer structure where 2LPs, 4LPs and 5LPs are employed. Clearly, with

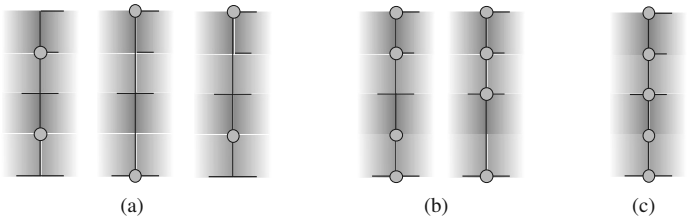

FIGURE 7 – *Four-layer laminated structure discretized with 2LPs (a), 4LPs (b) and 5LPs (c).*

this capability, the desired unknowns can be calculated in any interlaminar position.

4. Unified formulation for beam, plate and shell theories with Lagrange polynomials

Let us consider three beam, plate and shell multilayered structures as shown in Fig. 8. For the 1D model, the cross-section Ω lays on the x,z plane of a Cartesian reference system. As a consequence, the beam axis is placed along the y direction. The 2D plate model uses the z coordinate for the thickness direction and the shell adopts a curvilinear reference frame (α, β, z) to account for the curvature, where α and β are the two in-plane directions. In this paper, cylindrical shell structures are considered.
The displacement vector for the three models is introduced in the following :

$$\begin{array}{lcl} \mathbf{u}(x,y,z) & = & \{u_x \quad u_y \quad u_z\}^{\mathrm{T}} \\ \mathbf{u}(\alpha,\beta,z) & = & \{u_\alpha \quad u_\beta \quad u_z\}^{\mathrm{T}} \end{array} \tag{11}$$

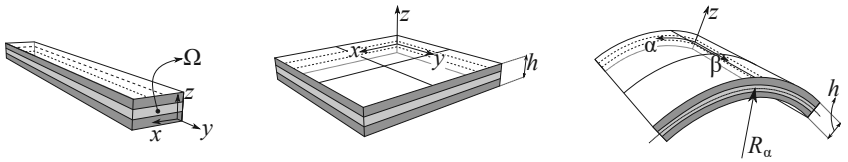

FIGURE 8 – *The modelling of generic composite structures using 1D and 2D plate and shell models. A Cartesian reference system is employed for the 1D beam and 2D plate model (x, y, z), whereas a curvilinear system (α, β, z) is used for the 2D shell model. For 1D model, y is the direction of the beam axis, and for the 2D models z is the thickness coordinate.*

where T is the transpose operator. The first formula of Eq. (11) is valid for beams and plates, the second one for shells. The stress, **σ**, and strain, **ε**, components are expressed in vectorial form as follows:

$$\begin{aligned}\boldsymbol{\sigma} &= \{\sigma_{xx}\ \sigma_{yy}\ \sigma_{zz}\ \sigma_{xz}\ \sigma_{yz}\ \sigma_{xy}\}^{\mathrm{T}},\ \boldsymbol{\varepsilon} = \{\boldsymbol{\varepsilon}_{xx}\ \boldsymbol{\varepsilon}_{yy}\ \boldsymbol{\varepsilon}_{zz}\ \boldsymbol{\varepsilon}_{xz}\ \boldsymbol{\varepsilon}_{yz}\ \boldsymbol{\varepsilon}_{xy}\}^{\mathrm{T}} \\ \boldsymbol{\sigma} &= \{\sigma_{\alpha\alpha}\ \sigma_{\beta\beta}\ \sigma_{zz}\ \sigma_{\alpha z}\ \sigma_{\beta z}\ \sigma_{\alpha\beta}\}^{\mathrm{T}},\ \boldsymbol{\varepsilon} = \{\boldsymbol{\varepsilon}_{\alpha\alpha}\ \boldsymbol{\varepsilon}_{\beta\beta}\ \boldsymbol{\varepsilon}_{zz}\ \boldsymbol{\varepsilon}_{\alpha z}\ \boldsymbol{\varepsilon}_{\beta z}\ \boldsymbol{\varepsilon}_{\alpha\beta}\}^{\mathrm{T}}\end{aligned} \tag{12}$$

Since linear analysis is performed in this work, only the linear strain components are considered. Therefore, the displacement-strain relations are expressed as

$$\boldsymbol{\varepsilon} = \mathbf{b}\,\mathbf{u} \tag{13}$$

where **b** is the matrix of differential operators. It changes according to the employed mathematical model and more information can be found in [49, 50].

As far as the constitutive relation is concerned, linear elastic orthotropic materials are considered in this work. Consequently, the constitutive relation reads as:

$$\boldsymbol{\sigma} = \mathbf{C}\,\boldsymbol{\varepsilon}, \tag{14}$$

where **C** is the material elastic matrix, whose explicit form can be found in [51, 52]. The 3D displacement field $\mathbf{u}(x,y,z)$ of the 1D beam, 2D plate and

shell models, within the framework of CUF, can be expressed as follows :

$$\begin{array}{lllll}
\text{1D BEAM :} & \mathbf{u}(x,y,z) & = & F_\tau(x,z)\mathbf{u}_\tau(y) & \\
& \delta\mathbf{u}(x,y,z) & = & F_s(x,z)\delta\mathbf{u}_s(y) & \\
\text{2D PLATE :} & \mathbf{u}(x,y,z) & = & F_\tau(z)\mathbf{u}_\tau(x,y), & \tau = 1,2,....,M \\
& \delta\mathbf{u}(x,y,z) & = & F_s(z)\delta\mathbf{u}_s(x,y), & s = 1,2,....,M \\
\text{2D SHELL :} & \mathbf{u}(\alpha,\beta,z) & = & F_\tau(z)\mathbf{u}_\tau(\alpha,\beta) & \\
& \delta\mathbf{u}(\alpha,\beta,z) & = & F_s(z)\delta\mathbf{u}_s(\alpha,\beta) &
\end{array} \tag{15}$$

It is clear that each theory can be easily obtained from Eq. (15) by using polynomials of different orders as F_τ and F_s. The expansion function used in this paper is based on Lagrange polynomials, which general relation is written as :

$$F_m(z) = \prod_{l=0, j\neq m}^{n} \frac{z-z_l}{z_m-z_l} = \frac{(z-z_0)\ldots(z-z_{m-1})\ldots(z-z_n)}{(z_m-z_0)\ldots(z_m-z_{m-1})(z_m-z_{m+1})\ldots(z_m-z_n)} \tag{16}$$

where n is the total number of LPs, m is the LP in which the formula is calculated and l are the other LPs. Obviously, to obtain polynomials of degree $n+1$, n LPs are needed. This formulation allows to arbitrarily change the position of LPs in the section (see Fig. 9).

For 1D structures, bi-dimensional functions discretize the cross-section. In

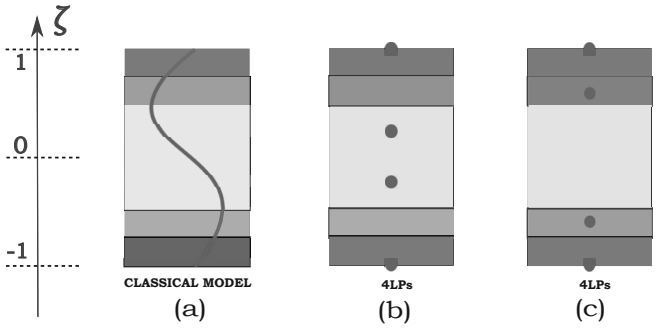

FIGURE 9 – *Through-the-thickness discretization of a multilayered structures using a classical model (a) and two different placement of 4LPs (b, c).*

this work three types of LPs placements are used : four LPs ensure a bi-linear interpolation, nine LPs a quadratic interpolation and sixteen LPs a cubic inter-

polation. For instance, if a quadratic interpolation is employed, the interpolation functions for the 1D beam models are :

$$\begin{aligned} F_\tau &= \frac{1}{4}(r^2+rr_\tau)(s^2+ss_\tau) && \tau = 1,3,5,7 \\ F_\tau &= \frac{1}{2}s_\tau^2(s^2-ss_\tau)(1-r^2)+\frac{1}{2}r_\tau^2(r^2-rr_\tau)(1-s^2) && \tau = 2,4,6,8 \\ F_\tau &= (1-r^2)(1-s^2) && \tau = 9 \end{aligned} \tag{17}$$

where r and s vary from -1 to $+1$, whereas r_τ and s_τ are the coordinates of the LPs. [2]

For 2D structures six different one-dimensional interpolations have been adopted, from 2 to 7 LPs, and the position of points was changed. As an example, the cubic interpolation using 4LPs is detailed hereafter. As shown in Fig. 9, the external LPs are located at $z=-1$ and $z=+1$, respectively, whereas the inner ones can be moved over the domain. The four equations at each LP are written as :

$$\begin{aligned} F_1 &= \frac{1}{(-2)(1+z_2)(1+z_3)}(z^3-(1+z_2+z_3)z^2+(z_2+z_3+z_2z_3)z-z_2z_3) \\ F_2 &= \frac{1}{(z_2+1)(z_2-z_3)(z_2-1)}(z^3-z_3z^2-z+z_3) \\ F_3 &= \frac{1}{(z_3+1)(z_3-z_2)(z_3-1)}(z^3-z_2z^2-z+z_2) \\ F_4 &= \frac{1}{(2)(1-z_2)(1-z_3)}(z^3+(1-z_2-z_3)z^2+(-z_2-z_3+z_2z_3)z+z_2z_3) \end{aligned} \tag{18}$$

5. Finite Element Approximation

The Finite Element Method (FEM) is adopted to discretise the *generalized* displacements $\mathbf{u}_\tau$ and the *generalized* variations $\delta\mathbf{u}_s$. Thus, recalling Eq. (15),

[2] Equation (17) is written in the natural coordinate system, see [50] for more details.

they are approximated as follows

$$\begin{array}{lllll}
\text{1D BEAM :} & \mathbf{u}_\tau(y) & = & N_i(y)F_\tau(x,z)\mathbf{u}_{\tau i} & \\
& \delta\mathbf{u}_s(y) & = & N_j(y)F_s(x,z)\delta\mathbf{u}_{sj} & \\
\text{2D PLATE :} & \mathbf{u}_\tau(x,y) & = & N_i(x,y)F_\tau(z)\mathbf{u}_{\tau i}, & i=1,2,....,N_n \\
& \delta\mathbf{u}_s(x,y) & = & N_j(x,y)F_s(z)\mathbf{u}_{sj}, & j=1,2,....,N_n \\
\text{1D SHELL :} & \mathbf{u}_\tau(\alpha,\beta) & = & N_i(\alpha,\beta)F_\tau(z)\delta\mathbf{u}_{\tau i} & \\
& \delta\mathbf{u}_s(\alpha,\beta) & = & N_j(\alpha,\beta)F_s(z)\delta\mathbf{u}_{sj} &
\end{array} \tag{19}$$

where N_i and N_j stand for the shape functions, the repeated subscripts i and j indicate summation, N_n is the number of the FE nodes per element and $\mathbf{u}_{\tau i}$ and $\mathbf{u}_{sj}$ are the following vectors of the FE nodal parameters :

$$\begin{array}{lll}
\mathbf{u}_{\tau i} & = & \left\{u_{x_{\tau i}}\ u_{y_{\tau i}}\ u_{z_{\tau i}}\right\}^T \\
\delta\mathbf{u}_{sj} & = & \left\{\delta u_{x_{sj}}\ \delta u_{y_{sj}}\ \delta u_{z_{sj}}\right\}^T
\end{array} \tag{20}$$

For the sake of brevity, the shape functions N_i and N_j are not reported here. They can be found in many reference texts, for instance, in Bathe [51]. However, it should be underlined that the choice of the expansion functions F_τ and F_s is completely independent of the choice of the beam Finite Element (FE) to be used along the beam axis. In this work, when using 1D beam models, classical one-dimensional FEs with four-node (B4) are adopted, i.e. cubic approximation along the y axis is assumed. For the 2D plate and shell models, classical 2D nine-node bi-quadratic FEs (Q9) are adopted for the shape function in the x,y and α,β planes, respectively.

For a better understanding of the proposed models, Fig. 10 shows the approximations previously explained for generic composite structures adopting 1D beam, 2D plate and shell. In particular, the expansion functions F_τ, used to approximate the cross-section of the 1D model and the thickness of the 2D models, and the shape functions N_i for the beam axis and the 2D in-plane approximation, are reported.

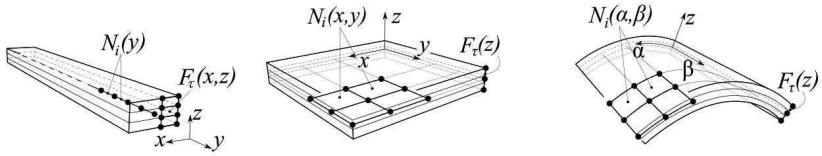

FIGURE 10 – *Mathematical models of the 1D beam , 2D plate and shell of generic composite structures.*

According to LM, the principle of virtual displacements shown in Eq. (2) can be written as :

$$\int_{V_k} (\delta\varepsilon^T \sigma) \mathrm{d}V_k \quad = \quad \delta L_{ext} \tag{21}$$

where k indicates the layer and V_k is the integration domain. Introducing the geometrical relations (Eq. (13)), the constitutive equation (Eq. (14)), and applying CUF (Eq. (15)) and FEM (Eq. ((19)), the following governing equations are obtained :

$$\delta \mathbf{u}^k_{sj} : \ \mathbf{K}^{kij\tau s} \, \mathbf{u}^k_{\tau i} = \mathbf{P}^k_{sj} \tag{22}$$

where $\mathbf{K}^{kij\tau s}$ is a 3×3 matrix, called fundamental nucleus (FN) of the mechanical stiffness matrix. The nucleus is the basic building block from which the stiffness matrix of the whole structure is computed. In fact, the construction of the stiffness matrix is formally identical and the explicit form of the elements of FN depends on the adopted formulation. For more information, see the works of Carrera *et al.* [53, 54]. The fundamental nucleus is expanded on the indexes τ and s to obtain the stiffness matrix of each layer k. Then, the matrices of each layer are assembled at the multi-layer level depending on the considered approach. $\mathbf{P}_{sj}$ is a 3×1 array, and it represents the fundamental nucleus of the external load. Its explicit expression is not given here for the sake of brevity, but it can be found in [53, 50] in the case of different loadings.

6. Benchmarks Description

To highlight the capabilities of the proposed ESL FEs based on Lagrange polynomials, four well-known benchmark problems are considered, and they are described hereafter. They regard a beam with two layers (both composite and bi-metallic cases are considered), a three-layer plate, a five-layer sandwich plate and a cylindrical shell.

B1 : Two-layer beam

Geometric description							
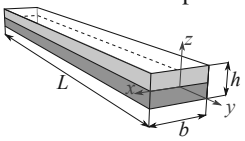							
L/h = 20 and h/b = 0.5							
Orthotropic material							
E_L/E_T	E_3/E_T	ν_{LT}	ν_{T3}	ν_{L3}	G_{LT}/E_T	G_{T3}/E_T	G_{L3}/E_T
25	1	0.25	0.25	0.25	0.5	0.2	0.2
with stacking sequence : [0°/90°]							
Bimetallic isotropic materials							
Bottom layer : E_1=210GPa, ν_1=0.3 ; Top layer : E_2=75GPa, ν_2=0.3							

Table 1 – B1: Geometrical and material loading properties of the two-layer beam. The reference solution comes from a refined LW model.

The first analysis case is a two-layer beam, as shown in Table 1. The beam is clamped and two different configurations of materials are considered, orthotropic and bi-metallic. The structure is loaded in the transverse z direction by a constant distributed pressure applied at the top of the beam. The pressure has a value of 1000 Pa. The transverse displacement at the tip and two stresses at the midspan are considered. The reference solution comes from a refined LW model.

B2 : Three-layer composite plate

A composite symmetric three-layer plate was analysed as the second example, and its geometric and loading conditions are described in Table 2. The plate is simply supported on its longitudinal edges and it is loaded with a transverse sinusoidal pressure $p = P_z \sin\left(\frac{\pi x}{b}\right)$, with $P_z = 1Pa$. The analysis was originally proposed by Pagano [55] and further investigated by Carrera [56].

B3 : Five-layer composite sandwich plate

A five-layer composite sandwich plate was further analysed. The geometric and loading conditions are described in Table 3. The plate is simply supported and it is loaded with a transverse bi-sinusoidal pressure $p = P_z \sin\left(\frac{\pi x}{a}\right)\sin\left(\frac{\pi y}{a}\right)$, with $P_z = 1000Pa$. This study case is taken from [57] and [58].

Geometric quantities							
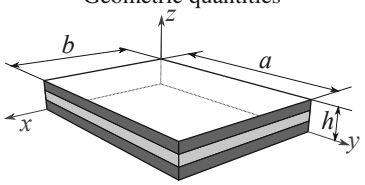							
b/h = 4 and 10 and a/b = 3							
Material							
E_L/E_T	E_3/E_T	ν_{LT}	ν_{T3}	ν_{L3}	G_{LT}/E_T	G_{T3}/E_T	G_{L3}/E_T
25	1	0.25	0.25	0.25	0.5	0.2	0.5
Stacking sequence							
Three equal layers : [0°/90°/0°]							
Non-dimensional displacements and stresses							
$\overline{w} = \frac{100\, E_T\, w}{\left(\frac{b^4}{h^4}\right) h\, P_z}$ $\quad \overline{\sigma}_{xx} = \frac{\sigma_{xx}}{\left(\frac{b}{h}\right)^2 P_z}$ $\quad \overline{\sigma}_{xz} = \frac{\sigma_{xz}}{\left(\frac{b}{h}\right) P_z}$							

Table 2 – B2: Geometrical and material properties of the three-layer composite plate. The study case is taken from [55].

Geometric quantities								
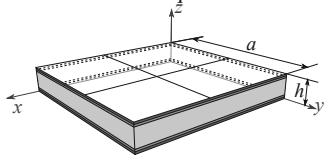								
a/h = 100, a = b, $h_{Core} = 8mm$, $h_{Skins} = 1mm$								
Material 1 (Skins)								
E_L [GPa]	E_3 [GPa]	E_T [GPa]	ν_{LT}	ν_{T3}	ν_{L3}	G_{LT} [GPa]	G_{T3} [GPa]	G_{L3} [GPa]
50	10	10	0.25	0.25	0.25	5	5	5
Material 2 (Core)								
E_L [MPa]	E_3 [MPa]	E_T [MPa]	ν_{LT}	ν_{T3}	ν_{L3}	G_{LT} [MPa]	G_{T3} [MPa]	G_{L3} [MPa]
0.01	75.85	0.01	0.25	0.25	0.25	22.5	22.5	22.5
Stacking sequence								
Bottom skins : [0°/90°], Top skins : [90°/0°] (each layer has the same thickness)								
Non-dimensional displacements and stresses								
$\overline{w} = \frac{100\, w\, E_T\, h^3}{P_z\, a^4}$ $\quad \overline{\sigma}_{xx} = \frac{\sigma_{xx}}{P_z\left(\frac{a}{h}\right)^2}$ $\quad \overline{\sigma}_{xz} = \frac{\sigma_{xz}}{P_z\left(\frac{a}{h}\right)}$								

Table 3 – B3: Geometrical and material properties of the five-layer composite sandwich plate under distributed bi-sinusoidal. The study case is taken from [57].

B4 : Three-layer composite shell

Geometric quantities							
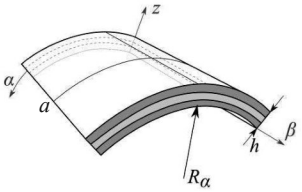							
$R_\alpha/b = \pi/3$, $R_\alpha/h = 10$ and $a = 1$							
Material							
E_L/E_T	E_3/E_T	ν_{LT}	ν_{T3}	ν_{L3}	G_{LT}/E_T	G_{T3}/E_T	G_{L3}/E_T
25	1	0.25	0.25	0.25	0.5	0.2	0.5
Staking sequence							
Three equal layers : [0°/90°/0°]							
Non-dimensional displacements and stresses							
$\overline{w} = \frac{10\,E_T\,w}{P_z\,h\left(\frac{R_\beta}{h}\right)^4}$ $\quad$ $\overline{\sigma}_{\beta\beta} = \frac{\sigma_{\beta\beta}}{P_z\left(\frac{R_\beta}{h}\right)^2}$ $\quad$ $\overline{\sigma}_{\beta z} = \frac{\sigma_{\beta z}}{P_z\left(\frac{R_\beta}{h}\right)}$							

Table 4 – B4: Geometrical and material properties of the three-layer composite shell. The study case is taken from [54].

As a final study case, a cylindrical shell was considered. The geometric properties and loading conditions are reported in Table 4. The shell is simply supported on its longitudinal edges and it is loaded with a transverse sinusoidal pressure $p = P_z \sin\left(\frac{\pi x}{b}\right)$ at the top position, with $P_z = 1Pa$. The analysis was originally proposed by Ren [59] and further investigated by Carrera [54].

7. Results for ESL Lagrange solutions

The benchmark problems were analyzed numerically and the results are shown in this section. Beam, plate and shell models are used for the static analyses, and values of displacement, axial and shear stress at particular points are calculated and compared with literature and reference results.

B1 : Two-layer beam Preliminary convergence analyses were carried out to set the reference solutions with the LW approach. Both transverse displacements at the tip section and shear stresses at the mid-span were studied. As a consequence, seven B4 FEs on the beam axis were chosen for the cross-ply beam

(see Fig. 11 (a)), whereas twenty B4 elements were adopted for the bi-metallic case (see Fig. 11 (b)). The converged model was used to evaluate displace-

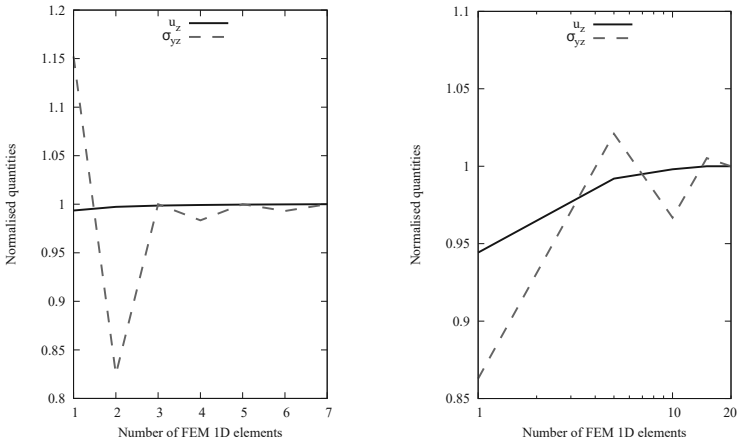

FIGURE 11 – *B1 : Convergence analyses for the two-layer composite (a) and bi-metallic (b) beam.*

Model	$-u_z$	σ_{yy}	σ_{yz} H	σ_{yz} I	DOF
LW(Ref.)	5.263	90.33	23.00	23.04	1848
TBM	5.265	92.38	10.02	23.20	305
EBBM	5.140	92.96	—	23.14	183
LP16	5.240	91.43	15.44	23.05	1056
LP9	5.233	91.35	14.76	23.04	594
LP4	5.131	95.91	10.07	22.87	264

Table 5 – B1: Transverse displacement and shear stresses of two-layer composite beam. $-u_z$ is calculated at the free tip of the beam, σ_{yy} at the mid-span and σ_{yz} at the mid-span of the beam at $z = h/4$.

ment, axial and shear stress components. The results are shown in Table 6 and Figs. 12 and 13. Clearly, a good accuracy for displacement and axial stress is obtained with every theory and LP position, whereas for the shear stress higher-order theories or integrated stresses have to be recalled.

B2 : Three-layer composite plate In this study case, two side-to-thickness

Model	$-u_z$	σ_{yy}	σ_{yz} H	σ_{yz} I	DOF
LW(Ref.)	0.2008	234.8	11.58	13.87	5124
TBM	0.2029	234.8	14.80	15.45	305
EBBM	0.2025	234.4	—	14.72	183
LP16	0.2008	234.7	14.71	13.87	2928
LP9	0.2006	234.9	11.54	13.71	1647
LP4	0.1629	234.8	14.79	14.59	732

Table 6 – B1: Transverse displacement and shear stresses of two-layer bimetallic beam. $-u_z$ is calculated at the free tip of the beam, σ_{yy} at the mid-span and σ_{yz} at the mid-span of the beam at $z = h/4$.

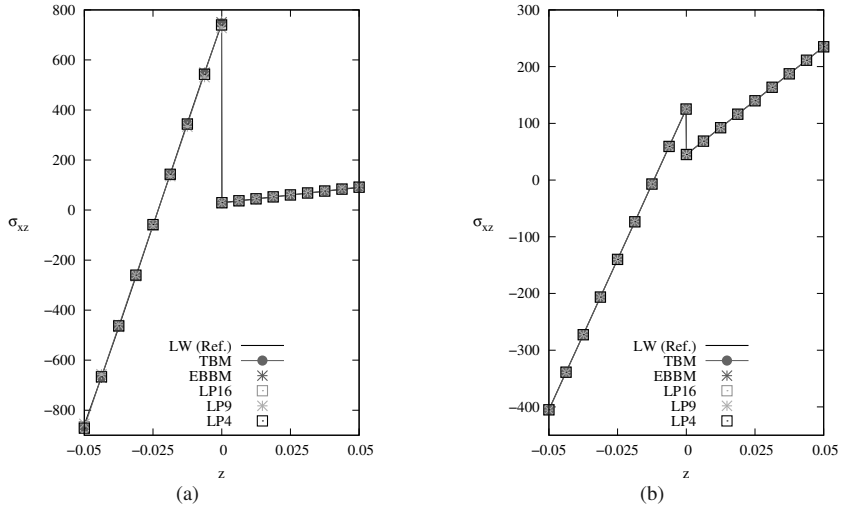

FIGURE 12 – *B1 : In-plane stress of clamped two-layer composite beam (a) and two-layer bimetallic beam (b).*

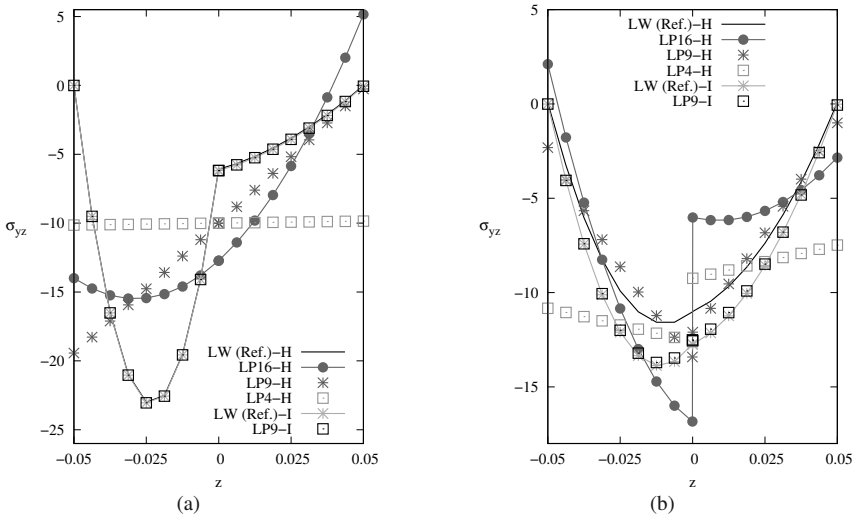

FIGURE 13 – *B1 : Shear stress of clamped two-layer composite beam (a) and two-layer bimetallic beam (b).*

ratios equal to 4 and 10 are considered. Transverse displacements, in-plane and shear stresses were studied using ESL Lagrange and comparing the results with the analytical reference solution from [55]. Regarding transverse displacements, some differences arise for each theory, especially for lower-order theories (as displayed in Table 7). Accurate results can be obtained for in-plane stresses (see Table 7 and Fig. 14) for both considered thicknesses. However, some issues are found for side-to-thickness ratio equal to 4 and LP3 and LP2. Considering shear stresses, critical issues can be seen, as displayed in Table 7 and Fig. 15. Using Hooke's Law, the results differ from the reference solution, even though LP6 and LP7 are closer to the analytical solution. This problem can be overcome if stress recovery is adopted (see Fig. 15).

B3 : Five-layer composite sandwich plate. For the third benchmark problem, a sandwich structure was considered to underline the potentialities and drawbacks of ESL approach. Accurate results for transverse displacements can be obtained at the top position (some issues surge only for low-order LP2 and LP3). However, it is not possible to obtain the same distribution as the reference solution (see Table 8 and Fig. 16 (a)), even if a higher number of LPs

b/h	4	10	4	10	4	10	
Model	$\overline{u}_z$		$\overline{\sigma}_{xx}$		$\overline{\sigma}_{xz}$ (H)		DOF
Ref.	2.820	0.919	1.176	0.725	0.358	0.420	—
FSDT	2.078	0.757	0.628	0.631	0.164	0.165	1085
CLT	0.504	0.504	0.627	0.629	—	—	651
LP7	2.704	0.888	1.130	0.724	0.327	0.388	4557
LP6	2.703	0.888	1.131	0.724	0.326	0.388	3906
LP5	2.652	0.867	1.130	0.718	0.289	0.315	3255
LP4	2.653	0.867	1.130	0.718	0.289	0.315	2604
LP3	2.057	0.753	0.653	0.628	0.162	0.164	1953
LP2	2.076	0.754	0.626	0.628	0.164	0.164	1302

Table 7 – B2: Transverse displacement, in-plane and shear stresses of simply supported three-layer composite plate under sinusoidal pressure. Comparison between different ratios *b/h*. $\overline{u}_z$ and $\overline{\sigma}_{xx}$ are calculated in the middle, σ_{xz} is calculated at *x/4*, *y/4*, *z/2*. Ref. solution comes from [55].

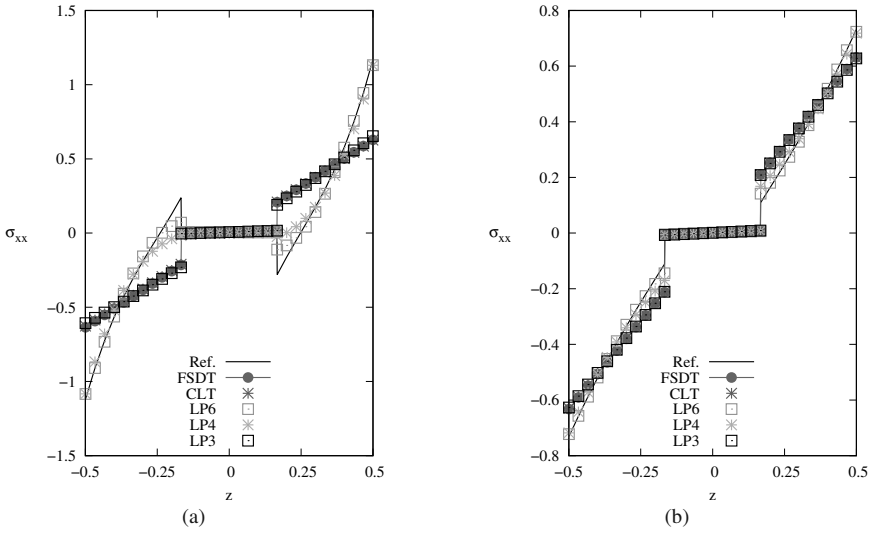

FIGURE 14 – *B2 : In-plane stresses for three-layer composite plate. b/h=4 (a) and b/h=10 (b) cases. Ref. solution comes from [55].*

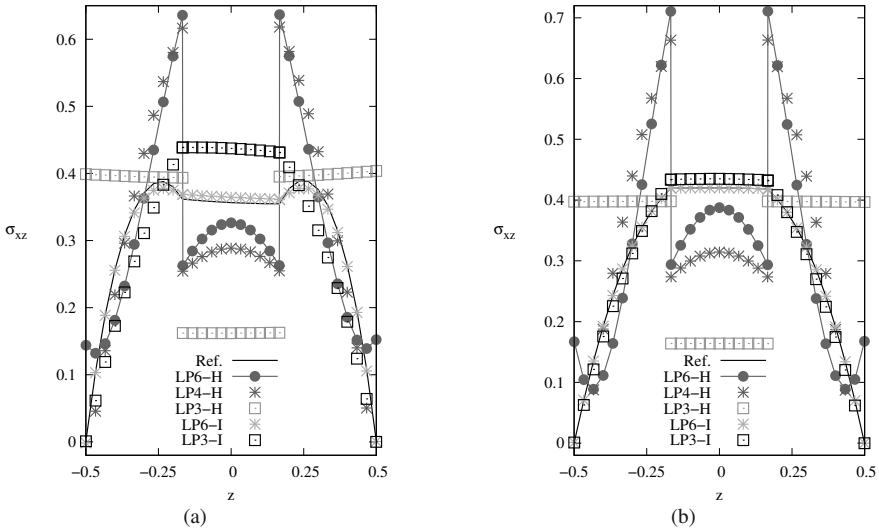

FIGURE 15 – *B2 : Shear stresses for three-layer composite plate. b/h=4 (a) and b/h=10 (b) cases. Ref. solution comes from [55].*

is employed. In Table 8 in-plane stresses are shown, and each theory leads to results close to the reference solution. Some problems arise when evaluating shear stresses, and using more LPs along the thickness can improve the solution (see Table 8 and Fig. 16 (b)), but the ESL is not capable of describing an accurate distribution within the skins. Thence, the ESL cannot evaluate the correct distribution over the thickness and a LW approach is compulsory.

B4 : Three-layer composite shell Finally, a shell study case was considered. Clearly, transverse displacements and in-plane stresses (shown in Table 9 and in Fig. 18 (a)) can be obtained with a good degree of precision, while increasing with the number of employed LPs.

Model	$\overline{w}$	$\overline{\sigma}_{xx}$	$\overline{\sigma}_{xz}$	DOF
Ref.	3.1167	-0.7819	0.1825	27783
FSDT	2.9330	-0.7955	0.0040	2205
CLT	2.9209	-0.7592	—	1323
LP7	3.1078	-0.7730	0.2290	9261
LP6	3.1078	-0.7727	0.2290	7938
LP5	3.0203	-0.7766	0.0918	6615
LP4	3.0203	-0.7765	0.0918	5292
LP3	2.9330	-0.7671	0.0041	3649
LP2	2.8127	-0.7629	0.0040	2646

Table 8 – B2: Transverse displacement, in-plane and shear stresses of the five-layer composite sandwich plate. $\overline{w}$ calculated in the middle of the plate at the top skin, $\overline{\sigma}_{xx}$ calculated in the middle of the plate at the bottom skin, $\overline{\sigma}_{xz}$ calculated at a quarter of the plate in the middle of the core. Ref. solution comes from [57].

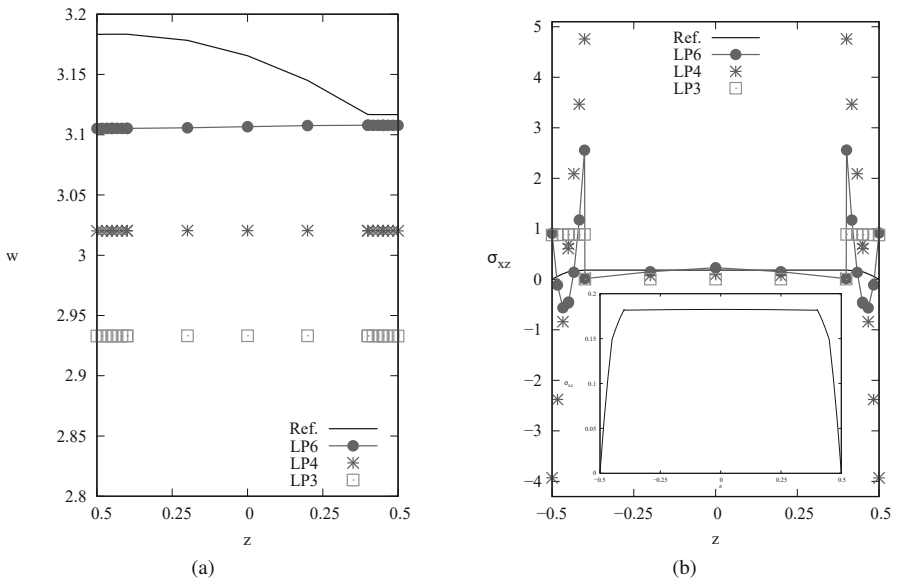

FIGURE 16 – *B3 : Transverse displacement (a) and shear stress (b) of five-layer composite sandwich. Ref. solution comes from [57].*

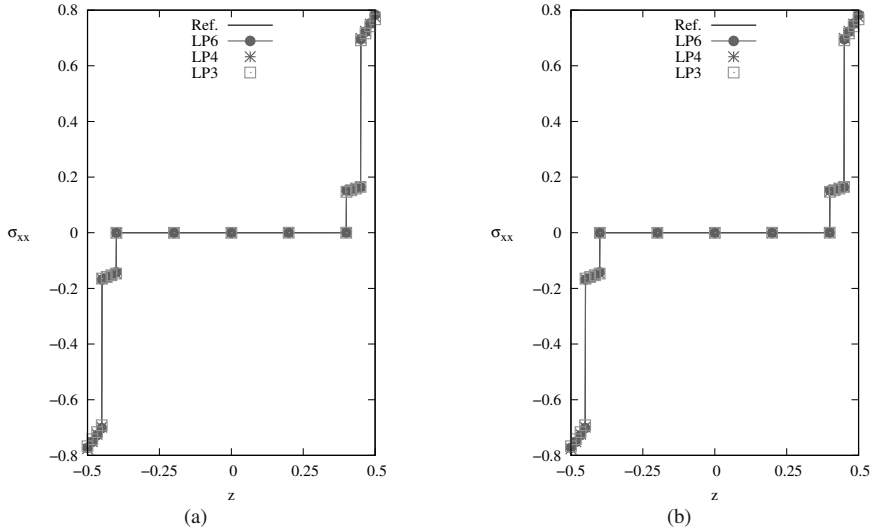

FIGURE 17 – *B3 : Transverse displacement (a) and shear stress (b) of five-layer composite sandwich. Ref. solution comes from [57].*

Model	$\overline{u}_z$	$\overline{\sigma}_{\beta\beta}$	$\overline{\sigma}_{\beta z}$ H	$\overline{\sigma}_{\beta z}$ I	DOF
Ref.	0.144	0.897	—	0.525	—
FSDT	0.112	0.721	0.184	0.519	875
CLT	0.076	0.709	—	0.500	525
LP7	0.139	0.875	0.476	0.527	3675
LP6	0.139	0.875	0.476	0.527	3150
LP5	0.136	0.868	0.382	0.533	2625
LP4	0.136	0.869	0.382	0.533	2100
LP3	0.119	0.766	0.196	0.545	1575
LP2	0.119	0.766	0.196	0.545	1050

Table 9 – B4: Transverse displacement, in-plane and shear stresses of simply supported three-layer composite shell under sinusoidal pressure. $\overline{u}_z$ calculated in the middle of the shell, $\overline{\sigma}_{\beta\beta}$ calculated in the middle of the shell at the top surface and $\overline{\sigma}_{\beta z}$ calculated at a quarter at the top surface. Ref. solution comes from [59].

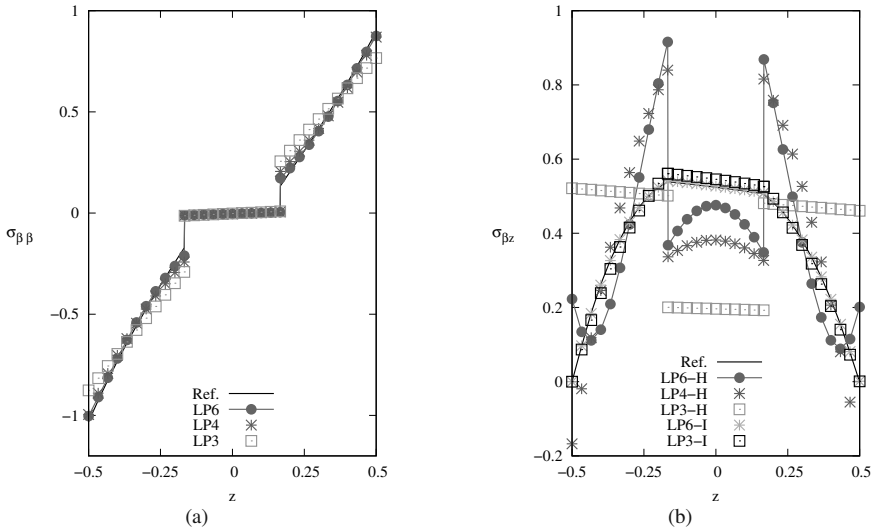

FIGURE 18 – *B4 : In-plane (a) and shear stress (b) of simply supported three-layer composite shell under sinusoidal pressure. Ref. solution comes from [59].*

As far as the shear stresses are considered (see Fig. 18 (b)), reliable results can be obtained in the middle point. However, the overall distribution is not as accurate as the reference one.

8. Special capabilities of Lagrange Expansion

The capability of the proposed ESL approach to deal with physical boundary conditions and global/local applications is proposed in this section with practical examples.

Physical boundary conditions on different nodes

This example shows how it is possible to decide the boundary conditions by using the Lagrange expansion in a general way. In Fig. 19, the cases of classical and Lagrange models are considered.

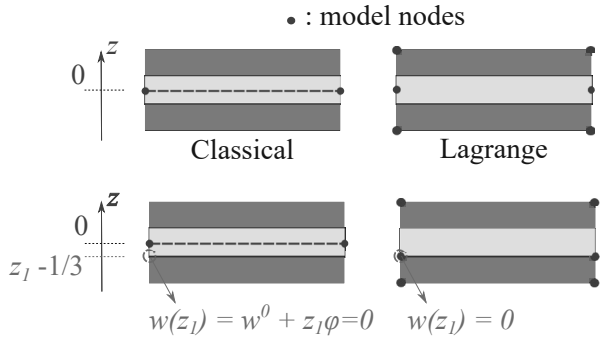

FIGURE 19 – *Computational models for Taylor and Lagrange (ESL approach) Expansions.*

Clearly, if boundary conditions have to be used to the middle line, both classical and Lagrange models can deal with it in an automatic manner. On the contrary, if the boundary conditions need to be applied at another point (in Fig. 19 at $z = 1/3$), classical models need to include an additional equation for the resolution of the problem, which is reported in Eq. (23).

$$w(z_1) = w^0 + z_1\phi = 0 \tag{23}$$

That additional equation can be included in the model using Lagrange multipliers, expressed by the following

$$\Pi = \lambda^{\mathrm{T}}\mathbf{Bq}$$

Thence, the following linear system has to be adopted.

$$\begin{bmatrix} \mathbf{K} & \mathbf{B}^{\mathrm{T}} \\ \mathbf{B} & \mathbf{0} \end{bmatrix} \begin{bmatrix} \mathbf{q} \\ \lambda \end{bmatrix} = \begin{bmatrix} \mathbf{F} \\ \mathbf{0} \end{bmatrix}$$

Thus, new unknowns have to be added to the displacement ones and the stiffness matrix has to be modified (for more information about Lagrange multipliers in CUF framework, interested readers are referred to [44]). This matrix also has the major drawback of not being necessarily positive definite and numerical problems can surge. On the contrary, Lagrange models can automatically include the boundary condition thanks to their capability to move the LPs, so it is necessary to have a point in correspondence of the desired location.
To highlight this capability, two different simply-supported conditions are considered (see figure 20). First, the condition is used at the bottom layer at

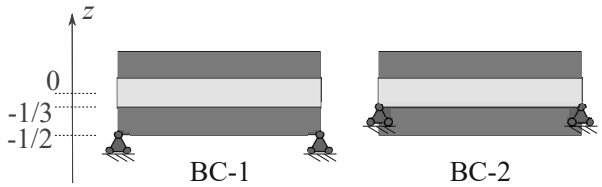

FIGURE 20 – *Scheme of two different boundary conditions used for three-layer composite plate to demonstrate the capabilities of LPs.*

$z = -1/2$ over the longitudinal edge. The second one is used at the interface layer at $z = -1/3$. The ESL theories are compared with LW reference theory in Tab. 10 and it can be seen how results can be obtained for both conditions, without losing accuracy with respect to the LW model. In particular, good results

Conditions		BC-1			BC-2		
Model	DOF	$\overline{u}_z$	$\overline{\sigma}_{xx}$	$\overline{\sigma}_{xz}$	$\overline{u}_z$	$\overline{\sigma}_{xx}$	$\overline{\sigma}_{xz}$
LW(Ref.)	12369	0.617	0.656	0.307	0.611	0.655	0.307
LP7	4557	0.610	0.656	0.281	0.604	0.655	0.281
LP6	3906	0.610	0.653	0.281	0.604	0.653	0.281
LP5	3255	0.604	0.653	0.224	0.579	0.652	0.224
LP4	2604	0.604	0.652	0.224	0.579	0.652	0.224
LP3	1953	0.573	0.628	0.115	0.568	0.628	0.115

Table 10 – Transverse displacement, in-plane and shear stresses of simply supported three-layer composite plate (aspect ratio equals to 20). Comparison between different boundary conditions used. $\overline{u}_z$ and $\overline{\sigma}_{xx}$ are calculated in the middle, $\overline{\sigma}_{xz}$ is calculated at x/4, y/4, z/2, see Table 2 for the adopted nondimensional values. LW in composed of six LP4.

are obtained for transverse displacements and in-plane stresses.

Global/Local method with ESL Lagrange for sandwich plate

An application of the capability of the Lagrange models of using different boundary conditions (see Fig. 19) is a single-step global/local approach. When dealing with different mathematical models, the main issue is to connect the two domains. Figure 21 describes this issue. In particular, Fig. 21(a) displays LW and classical domains and due to the difference of the mathematical approaches, four additional equations have to be added to the system of equation (similarly to what is shown in Fig. 19 and Eq. (23)). For instance, Carrera *et al.*

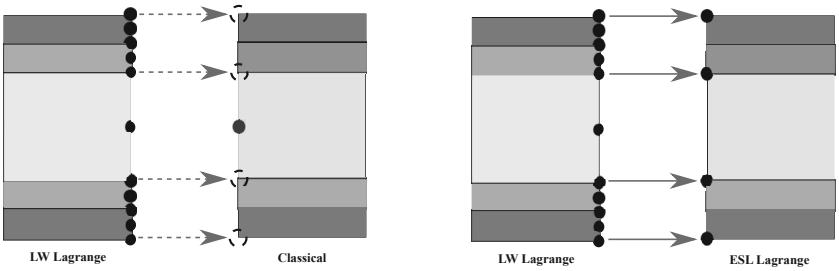

FIGURE 21 – *Example of joining different structural domains. Between classical and LW Lagrange-based zones, there are no connection points (a), whereas one can opportunely choose the position of LPs to join different domains (b).*

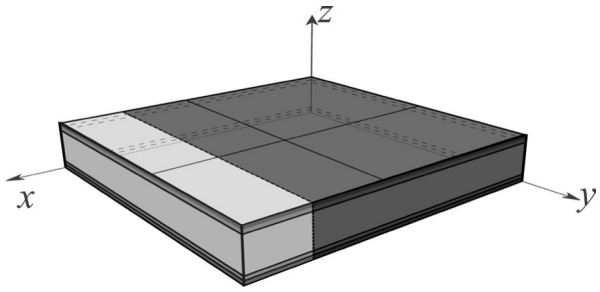

FIGURE 22 – *Example of the single-step global/local approach applied to the five-layer sandwich plate. ESL approach was used in the dark grey part and the LW approach in the light grey part.*

[44, 45, 50] used the Lagrange Multipliers to overcome this problem. On the contrary, the ESL models shown in this work, allows for the arbitrary use of LPs, so that a point-by-point connection can be ensured between the domains, as shown in Fig. 21(b). This procedure is hereafter applied on the five-layer composite sandwich plate, as illustrated in Fig. 22, where the ESL approach was used in the dark grey part and the LW approach in the light grey part. The results are shown in Table 11, where the upper scripts indicate the number of employed FEs. The capability to obtain accurate results is shown, especially for

Model	$\overline{w}$	$\overline{\sigma}_{xx}$	$\overline{\sigma}_{xz}$	DOF
LW	3.1167	-0.7819	0.1825	27783
LP6	3.1078	-0.7727	0.2290	7938
LP4	3.0203	-0.7765	0.0918	5292
LW$^{\times 20}$-LP6$^{\times 80}$	3.1150	-0.7829	0.1576	12663
LW$^{\times 30}$-LP6$^{\times 70}$	3.1180	-0.7758	0.1704	14553
LW$^{\times 20}$-LP4$^{\times 80}$	3.0367	-0.7725	0.1665	10647
LW$^{\times 30}$-LP4$^{\times 70}$	3.0510	-0.7624	0.1764	12789

Table 11 – Transverse displacement, shear and normal stresses of the fivelayer composite sandwich plate. $\overline{w}$ calculated in the middle of the plate at the top skin (ESL domain), $\overline{\sigma}_{xx}$ calculated in the middle of the plate at the bottom skin (ESL domain), $\overline{\sigma}_{xz}$ calculated at a quarter of the plate in the middle of the core. LW is composed of five LP5. Comparison with Global Local Solution.

the shear stresses, with fewer DOFs than the LW solution. In particular, transverse displacements and shear stresses for the combinations LW$^{\times 30}$-LP6$^{\times 70}$ LW$^{\times 30}$-LP4$^{\times 70}$ and LW are displayed in Fig. 23.

9. Conclusions

The present research work proposed Equivalent Single Layer Finite Elements based on the Lagrange polynomials for the static analysis of beams, plates and shells. One-dimensional beams and two-dimensional plate and shell models were built in the framework of the Carrera Unified Formulation. Four well-known case studies were taken from open literature, and the results obtained with the developed ESL FEs were compared with those from Layer-Wise models and references. The following main conclusions can be summarized:

1 ESL FE models based on Lagrange polynomials lead to increasingly accurate results, as the number of LPs increases, compared to LW models. This is true for both transverse displacements and in-plane stresses.

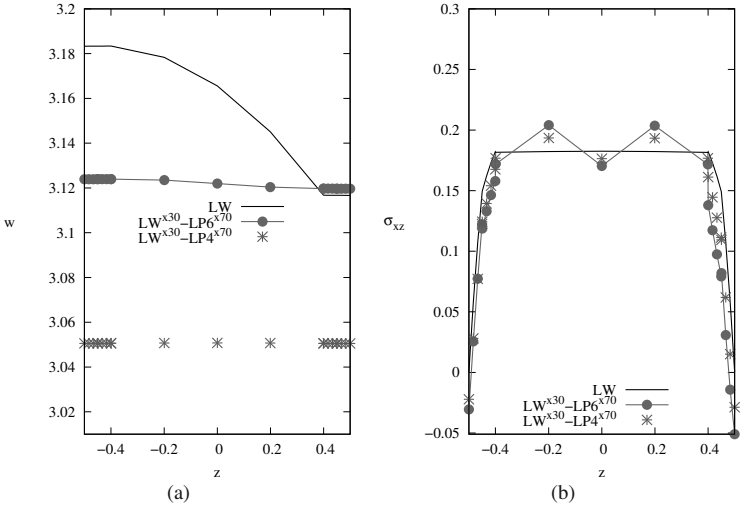

FIGURE 23 – *Transverse displacement (a) and shear stress (b) of five-layer composite sandwich. LW is composed of five LP5. Comparison with Global Local Solution.*

Less accurate results are obtained for shear components (unless they are evaluated integrating the three-dimensional (3D) indefinite equilibrium equations, rather than with Hooke's law).

2 The application of Lagrange Points (LPs) and the fact that unknowns are pure displacements allows implementing boundary conditions which are closer to the ones used in practical applications.

3 The use of Lagrange polynomials leads to a single-step global/local procedure without implementing any additional constraint equation (as it happens in classical models). This method allows for an accurate evaluation of both in-plane and shear stresses when compared with LW models with a significant decrease of computational cost with respect to the use of traditional models and Lagrange multipliers.

Bibliography

[1] E. Carrera, *Historical review of zig-zag theories for multilayered plates and shells*, Applied Mechanics Review, 56(3), 2003, pp. 287-308.

[2] R.K. Kapania, S. Raciti, *Recent advances in analysis of laminated beams and*

plates. Part I: *Shear effects and buckling*, AIAA Journal, 27(7), pp. 923-935, 1989.

[3] R.K. Kapania and S. Raciti, *Recent advances in analysis of laminated beams and plates.* Part II: *Vibrations and wave propagation*, AIAA Journal, 27(7), 1989, pp. 935-946.

[4] J.N. Reddy and D.H. Robbins, *Theories and Computational Models for Composite Laminates*, Applied Mechanics Reviews, 47(6), 1994, pp. 147-169.

[5] E. Carrera, *Developments, ideas, and evaluations based upon reissner's mixed variational theorem in the modeling of multilayered plates and shells*, Applied Mechanics Review, 54(4), 2001, pp. 301-329.

[6] L. Euler, *Methodus inveniendi lineas curvas maximi minimive proprietate gaudentes sive solutio problematis isoperimetrici latissimo sensu accepti*, vol. 1. Springer Science & Business Media, Berlin 1952.

[7] S.P. Timoshenko, *On the transverse vibrations of bars of uniform cross section*, Philosophical Magazine, 43, 1922, pp. 125-131.

[8] V.V. Novozhilov, *Theory of elasticity*, Pergamon Press, Oxford 1961.

[9] V.Z. Vlasov, *Thin-walled elastic beams*, Office of Technical Services, US Department of Commerce, Washington DC 1961.

[10] R.D. Ambrosini, J.D. Riera, R.F. Danesi, *A modified vlasov theory for dynamic analysis of thin-walled and variable open section beams*, Engineering Structures, 22(8), 2000, pp. 890-900.

[11] I. Mechab, N. El Meiche, F. Bernard, *Analytical study for the development of a new warping function for high order beam theory*, Composites Part B: Engineering, 119, 2017, pp. 18-31.

[12] P.O. Friberg, *Beam element matrices derived from vlasov's theory of open thin-walled elastic beams*, International Journal for Numerical Methods in Engineering, 21(7), 1985, pp. 1205-1228.

[13] R. Schardt, *Eeine erweiterung der technischen biegetheorie zur berechnung prismatischer faltwerke*, Der Stahlbau, 35, 1966, pp. 161-171.

[14] N. Peres, R. Gonçalves, D. Camotim, *First-order generalised beam theory for curved thin-walled members with circular axis*, Thin-Walled Structures, 107, 2016, pp. 345-361.

[15] N. Silvestre, *Generalised beam theory to analyse the buckling behaviour of circular cylindrical shells and tubes*, Thin-Walled Structures, 45(2), 2007, pp. 185-198.

[16] G. Kirchhoff, *Über das gleichgewicht und die bewegung einer elastischen scheibe*, *Journal für die reine und angewandte Mathematik (Crelles Journal)*, 40, 1850, pp. 51-88.

[17] A.E.H. Love, *A treatise on the mathematical theory of elasticity*, Cambridge University Press, Cambridge 1927.

[18] E. Reissner and Y. Stavsky, *Bending and stretching of certain types of heterogeneous aeolotropic elastic plates*, Journal of Applied Mechanics, 28, 1961, pp. 402-408.

[19] E. Reissner, *The effect of transverse shear deformation on the bending of elastic plates*, Journal of Applied Mechanics, 12, 1945, pp. 69-77.

[20] R. Mindlin, *Influence of rotary inertia and shear flexural motion of isotropic, elastic plates*, Journal of Applied Mechanics, 18, 1951, pp. 31-38.

[21] J.N. Reddy, *A simple higher-order theory for laminated composite plates*, Journal of Applied Mechanics, 51, 1984, pp. 745-752.

[22] E. Carrera, *Evaluation of layerwise mixed theories for laminated plates analysis*, AIAA Journal, 36(5), 1998, pp. 830-839.

[23] F.G. Rammerstorfer, K. Dorninger, A. Starlinger, *Composite and sandwich shells*, in F.G. Rammerstorfer, *Nonlinear analysis of shells by finite elements*, Springer, 1992, pp. 131-194.

[24] J.N. Reddy, *An evaluation of equivalent-single-layer and layerwise theories of composite laminates*, Composite structures, 25(1-4), 1993, pp. 21-35.

[25] A.S. Mawenya and J.D. Davies, *Finite element bending analysis of multilayer plates,* International Journal for Numerical Methods in Engineering, 8(2), 1974, pp. 215-225.

[26] A.K. Noor and W.S. Burton, *Assessment of computational models for multilayered composite shells*, Applied Mechanics Reviews, 43, 1990, pp. 67-97.

[27] E. Carrera, *A class of two-dimensional theories for anisotropic multilayered plates analysis*, Memorie dell'Accademia delle Scienze di Torino. Classe di Scienze Fisiche, Matematiche e Naturali, 19-20, 1995-96, pp. 49-57.

[28] E. Carrera and A. Robaldo, *Extension of Reissner mixed variational principle to thermopiezelasticity*, Atti dell'Accademia delle Scienze di Torino. Classe di Scienze Fisiche, Matematiche e Naturali, 141, 2007, pp. 3-18.

[29] A.S.D. Wang and F.W. Crossman, *Calculation of edge stresses in multilayer laminates by sub-structuring*, Journal of Composite Materials, 12(1), pp. 76-83, 1978.

[30] N.J. Pagano and S.R. Soni, *Global-local laminate variational model*, International Journal of Solids and Structures, 19(3), 1983, pp. 207-228.

[31] R. Jones, R. Callinan, K.K. Teh, K.C. Brown, *Analysis of multi-layer laminates using three-dimensional super-elements*, International Journal for Numerical Methods in Engineering, 20(3), 1984, pp. 583-587.

[32] M.B. Dehkordi, M. Cinefra, S.M.R. Khalili, E. Carrera, *Mixed LW/ESL*

models for the analysis of sandwich plates with composite faces, Composite Structures, 98, 2013, pp. 330-339.

[33] E. Carrera and S. Valvano, *Analysis of laminated composite structures with embedded piezoelectric sheets by variable kinematic shell elements*, Journal of Intelligent Material Systems and Structures, 28(20), 2017, pp. 2959-2987.

[34] A. Pagani, E. Carrera, R. Augello, D. Scano, *Use of Lagrange polynomials to build refined theories for laminated beams, plates and shells*, Composite Structures, 276, 2021, p. 114505.

[35] E. Carrera, G.A. Fiordilino, M. Nagaraj, A. Pagani, M. Montemurro, *A global/local approach based on cuf for the accurate and efficient analysis of metallic and composite structures*, Engineering Structures, 188, 2019, pp. 188-201.

[36] K.M. Mao and C.T. Sun, *A refined global-local finite element analysis method*, International Journal for Numerical Methods in Engineering, 32(1), 1991, pp. 29-43.

[37] E. Carrera, A. Garcia de Miguel, G.A. Fiordilino, A. Pagani, *Global/local analysis of free-edge stresses in composite laminates*, in AIAA Scitech 2019 Forum, pp. 1-7.

[38] E. Carrera, A.G. de Miguel, M. Filippi, I. Kaleel, A. Pagani, M. Petrolo, E. Zappino, *Global-local plug-in for high-fidelity composite stress analysis in Femap/NX Nastran*, Mechanics of Advanced Materials and Structures, 28(11), 2021 pp. 1121-1127.

[39] H.B. Dhia, *Problèmes mécaniques multi-échelles: la méthode arlequin*, Comptes Rendus de l'Académie des Sciences – Series IIB – Mechanics-Physics-Astronomy, 326(12), 1998, pp. 899-904.

[40] H.B. Dhia and G. Rateau, *The arlequin method as a flexible engineering design tool*, International journal for numerical methods in engineering, 62(11), 2005, pp. 1442-1462.

[41] F. Biscani, G. Giunta, S. Belouettar, E. Carrera, H. Hu, *Variable kinematic beam elements coupled via arlequin method*, Composite Structures, 93(2), 2011, pp. 697-708.

[42] F. Biscani, G. Giunta, S. Belouettar, E. Carrera, H. Hu, *Variable kinematic plate elements coupled via arlequin method*, International Journal for Numerical Methods in Engineering, 91(12), 2012, pp. 1264-1290.

[43] Q.Z. He, H. Hu, S. Belouettar, G. Guinta, K. Yu, Y. Liu, F. Biscani, E. Carrera, M. Potier-Ferry, *Multi-scale modelling of sandwich structures using hierarchical kinematics*, Composite Structures, 93(9), 2011, pp. 2375-2383.

[44] E. Carrera, A. Pagani, M. Petrolo, *Use of Lagrange multipliers to combine 1d variable kinematic finite elements*, Computers & Structures, 129, 2013, pp. 194-206.

[45] E. Carrera and E. Zappino, *Analysis of complex structures coupling variable kinematics one-dimensional models*, in ASME International Mechanical Engineering Congress and Exposition, volume 46421, pp. 1-8. American Society of Mechanical Engineers, 2014.

[46] K. Washizu, *Variational methocs in elasticity and plasticity*, Pergamon Press, Oxford 1968.

[47] E. Carrera, *Transverse Normal Stress Effects in Multilayered Plates*, Journal of Applied Mechanics, 66(4), 1999, pp. 1004-1012.

[48] E. Carrera, M. Petrolo, *Refined beam elements with only displacement variables and plate/shell capabilities*, Meccanica, 47(3), 2012, pp. 537-556.

[49] E. Carrera, A. Pagani, S. Valvano, *Shell elements with through-the-thickness variable kinematics for the analysis of laminated composite and sandwich structures*, Composites Part B: Engineering, 111, 2017, pp. 294-314.

[50] E. Carrera, M. Cinefra, M. Petrolo, E. Zappino, *Finite element analysis of structures through unified formulation*, John Wiley & Sons, Hoboken, New Jersey 2014.

[51] K.J. Bathe, *Finite Element Procedure*, Prentice hall, Upper Saddle River, New Jersey 1996.

[52] T.J.R. Hughes, *The Finite Element Method: Linear Static and Dynamic Finite Element Analysis,* Courier Corporation, Chelmsford, Massachusetts 2012.

[53] E. Carrera, G. Giunta, M. Petrolo, *Beam structures: classical and advanced theories*, John Wiley & Sons, Hoboken, New Jersey 2011.

[54] E. Carrera, *Theories and finite elements for multilayered plates and shells: a unified compact formulation with numerical assessment and benchmarking,* Archives of Computational Methods in Engineering, 10(3), 2003, pp. 215-296.

[55] N.J. Pagano, *Exact solutions for composite laminates in cylindrical bending*, Journal of Composite Materials, 3(3), 1969, pp. 398-411.

[56] E. Carrera, *Single* vs *multilayer plate modelings on the basis of Reissner's mixed theorem*, Aiaa Journal-AIAA J, 38, 2000, pp. 342-352.

[57] A. Pagani, S. Valvano, and E. Carrera, *Analysis of laminated composites and sandwich structures by variable-kinematic MITC9 plate elements*, Journal of Sandwich Structures & Materials, 20(1), 2018, pp. 4-41.

[58] M. Petrolo and A. Lamberti, *Axiomatic/asymptotic analysis of refined layer-wise theories for composite and sandwich plates*, Mechanics of Advanced Materials and Structures, 23(1), 2016, pp. 28-42.

[59] J.G. Ren, *Exact solutions for laminated cylindrical shells in cylindrical bending*, Composites Science and Technology, 29(3), 1987, pp. 169-187.

Accademia
delle Scienze
di Torino
1783

Euro 15

ISSN: 2974-8291